

Cutaneous Feedback of Planar Fingertip Deformation and Vibration on a da Vinci Surgical Robot

Claudio Pacchierotti^{1,2,3}, Priyanka Shirsat³, Jacqueline K. Koehn³,
Domenico Prattichizzo^{1,2}, and Katherine J. Kuchenbecker³

¹Dept. of Information Engineering and Mathematics, University of Siena, Italy. ²Dept. of Advanced Robotics, Istituto Italiano di Tecnologia, Italy.

³Dept. of Mechanical Engineering and Applied Mechanics, Haptics Group, GRASP Laboratory, University of Pennsylvania, USA.

I. INTRODUCTION

Telerobotic surgical systems involve a slave robot, which interacts with the patient, and a master console, operated by the human surgeon. The slave robot reproduces the hand movements of the surgeon, who in turn needs to observe the operative environment with which the robot is interacting. The latter can be achieved by a combination of visual and haptic cues that flow from the operating table to the surgeon. Visual feedback is already available in commercial robotic surgery systems (e.g., the Intuitive Surgical da Vinci Si), but current surgical robots have very limited haptic feedback, despite its expected clinical benefits [1]. This omission is mainly due to the negative effect that haptic feedback has on the stability of the teleoperation loop. Haptic force feedback can in fact lead to undesired oscillations of the system, which interfere with the surgery and may be dangerous for the patient [2], [3].

In this respect, cutaneous feedback has recently received great attention in the haptics and medical research fields; delivering ungrounded sensory cues to the surgeon's skin conveys rich information and does not affect the stability of the teleoperation system [2], [4], [5]; Prattichizzo et al. [2] call this approach *sensory subtraction*, in contrast to *sensory substitution*, as it subtracts the kinesthetic part of the interaction to leave only the cutaneous cues. This paper presents a novel cutaneous feedback system for the da Vinci surgical robot, as shown in Fig. 1. Designed to provide planar fingertip deformation and vibration cues to the surgeon, our system is composed of a BioTac tactile sensor mounted to one of the robot's slave tools and a cutaneous display device attached to the corresponding master controller. Contact deformations and vibrations sensed by the BioTac are directly mapped to input commands for the cutaneous device's motors using a model-free data-driven algorithm. A preliminary version of the deformation part of the algorithm was presented in [6].

II. THE HAPTIC SYSTEM: SENSING AND ACTUATION

The BioTac tactile sensor mimics the physical properties and sensory capabilities of the human fingertip [7]. It consists of three complementary sensory systems (skin deformation, fluid pressure, and temperature) integrated into a single package. Contact forces deform the elastic skin and the underlying conductive fluid, changing the impedances of 19 electrodes distributed over the surface of the rigid core. Vibrations in the skin propagate through the fluid and are detected as AC signals by a hydro-acoustic pressure sensor, while this sensor's DC value indicates the steady-state pressure of the fluid. As shown in Fig. 1a, the BioTac sensor has been attached to the da Vinci slave robotic tool through a custom plastic nail.

The haptic tactile interface employed in this work is an

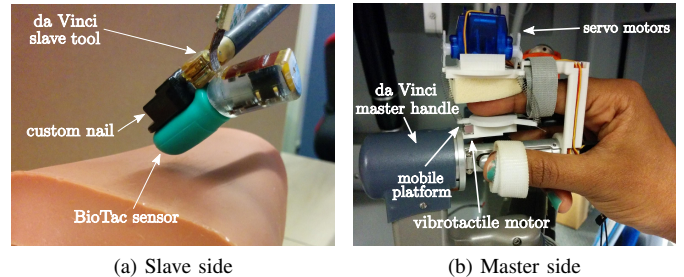


Fig. 1. System setup. A BioTac tactile sensor is attached to a da Vinci tool, and a cutaneous device is attached to the robot's corresponding master controller. The BioTac follows the motions of the operator's finger.

augmented 3-DoF fingertip cutaneous device, similar to the one presented in [8]. The device frame houses three servo motors and is rigidly attached to the grip interface of the da Vinci master controller as shown in Fig. 1b. The device fastens to the user's index finger with a strap between the PIP and DIP joints. A mobile platform holding one vibrotactile motor is suspended beneath the operator's fingertip by three cables; compression springs around the cables hold the mobile platform in a reference configuration away from the fingertip. By controlling the cable lengths, the servos orient and translate the mobile platform in three-dimensional space to apply planar deformations to the fingertip, while the vibrotactile motor conveys fingertip vibrations. The servo motors used in our prototype are Sub-Micro Servo 3.7 g motors (Pololu Corporation, USA), which are position controlled and can exert up to 39 N-mm torque. Our vibrotactile motor is a Forcereactor short-vibration feedback motor (Alps Electric, Japan).

III. MAPPING SENSED DATA TO MOTOR COMMANDS

Our goal is to enable the user to perceive, through the fingertip cutaneous device, the deformations and vibrations experienced by the BioTac as it interacts with the patient's tissue. In other words, we aim to find a good many-to-few mapping between the rich sensory information provided by the BioTac and the limited actuation capabilities of the fingertip cutaneous device. Let $s_c(k) \in \mathbb{R}^{20}$ be a vector containing the electrodes and DC pressure values at instant k . The BioTac senses these quantities at 100 Hz with a precision of 12 bits, and it senses AC pressure (vibrations) at 2200 Hz. In contrast, our cutaneous device uses three position-controlled servomotors and one vibrotactile motor. Let $m(k) \in \mathbb{R}^3$ be the commanded angles for the servomotors. Sampling time index k will be omitted from now on.

How can we map a given BioTac sensation to a congruent configuration of the mobile platform and signal input for

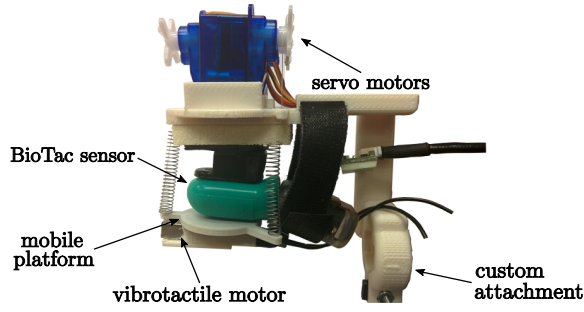


Fig. 2. Data collection. With the BioTac inside the device, we moved the mobile platform to a range of configurations and drove the vibrotactile motor with a variety of signals. These experiments tell us how each output affects what the BioTac feels, as a proxy for what the human fingertip feels.

the vibrotactile motor? Since the BioTac mimics the physical properties of the human fingertip [7], we placed it inside the cutaneous device, so that we could understand how the motion of the mobile platform affects the tactile sensor. Fig. 2 shows the data collection setup. We then moved the mobile platform to a wide range of configurations and registered the effect of each configuration on the BioTac, saving both the commanded motor angles \mathbf{m}_* and the resulting effect on the tactile sensor $\mathbf{s}_{c,*}$. Moreover, to understand how different platform configurations affect the way the BioTac feels vibrations, for each configuration we played a two-second-long swept sine wave (1 Hz – 1000 Hz) through the vibrotactile motor, and we registered its effect on the BioTac’s pressure sensor (AC signals). A moderate step size of 10° yields $\left(\frac{200^\circ - 30^\circ}{5^\circ}\right)^3 = 4913$ unique platform configurations.

A. Input signal for the servo motors

At the end of the data collection, we were able to evaluate the mapping function

$$\mu_c(\mathbf{s}_{c,*}) = \mathbf{m}_*, \quad (1)$$

which links the BioTac sensed data to the tested motor input commands. However, function $\mu_c(\cdot)$ is defined for a very small subset of all the possible tactile sensations the BioTac can experience. For this reason, we cannot simply deploy the sensor in a random remote environment and expect its sensed points to be in the domain of our mapping function. Unfortunately, this problem cannot be fixed by reducing the angle step size during data collection. The shape of the platform and the limited degrees of freedom of the cutaneous device will always couple the behavior of neighboring electrodes, so many tactile inputs that the BioTac can sense cannot be reached with the given device. We thus need a function that maps a *generic* sensed point \mathbf{s}_c to one in our mapping function’s domain. We solve this problem by looking for the point in our domain closest to the sensed one, and thus define

$$\nu_c(\mathbf{s}_c) = \mathbf{s}_{c,*}, \quad (2)$$

as the function that maps a generic point \mathbf{s}_c , sensed by the BioTac, to the closest one in the domain of our function $\mu_c(\cdot)$. In this work we implemented the nearest point search using the 20-dimensional Euclidean distance metric.

It is now trivial to combine functions $\mu_c(\cdot)$ and $\nu_c(\cdot)$ and define

$$f_c(\mathbf{s}_c) = \mu_c(\nu_c(\mathbf{s}_c)) = \mu_c(\mathbf{s}_{c,*}) = \mathbf{m}_*, \quad (3)$$

as the function that maps a generic point \mathbf{s}_c , sensed by the BioTac, to the motor angle triplet \mathbf{m}_* that most closely causes sensation \mathbf{s}_c .

B. Input signal for the vibrotactile motor

During data collection, we also estimated the transfer function between the vibrations sensed by the BioTac and the vibrotactile motor’s input signal for each platform configuration considered. We were thus able to define the mapping function

$$\mu_v(\mathbf{m}_*) = \mathbf{c}_*, \quad (4)$$

which links each tested angle triplet \mathbf{m}_* to the coefficients of the corresponding estimated transfer function. We considered a transfer function with 6 poles and 6 zeros, therefore $\mathbf{c}_* \in \mathbb{R}^{14}$.

Every time the algorithm described in Sec. III-A evaluates a motor angle triplet \mathbf{m}_* for the servomotors, the algorithm also retrieves the filter coefficients \mathbf{c}_* and filters the sensory information coming from the BioTac’s hydro-acoustic pressure sensor accordingly. For the sake of clarity, the complete algorithm is summarized below.

Algorithm 1: Tactile rendering algorithm

```

foreach instant  $k$  do
  read BioTac’s data  $\mathbf{s}_c$ 
  find nearest neighbor in  $\mu_c(\cdot)$  domain:  $\nu_c(\mathbf{s}) = \mathbf{s}_{c,*}$ 
  find corresponding motor angles:  $\mu_c(\mathbf{s}_{c,*}) = \mathbf{m}_*$ 
  find corresponding filter coefficients:  $\mu_v(\mathbf{m}_*) = \mathbf{c}_*$ 
  move servos to  $\mathbf{m}_*$ 
  send filtered signal to the vibrotactile motor
end

```

We are in the process of evaluating the described system through a human-subject experiment on palpation.

REFERENCES

- [1] L. Moody, C. Baber, and T. N. Arvanitis, “Objective surgical performance evaluation based on haptic feedback,” *Studies in health technology and informatics*, pp. 304–310, 2002.
- [2] D. Prattichizzo, C. Pacchierotti, and G. Rosati, “Cutaneous force feedback as a sensory subtraction technique in haptics,” *IEEE Trans. on Haptics*, vol. 5, no. 4, pp. 289–300, 2012.
- [3] N. Diolaiti, G. Niemeyer, F. Barbagli, and J. K. Salisbury, “Stability of haptic rendering: Discretization, quantization, time delay, and Coulomb effects,” *IEEE Trans. on Robotics*, vol. 22, no. 2, pp. 256–268, 2006.
- [4] L. Meli, C. Pacchierotti, and D. Prattichizzo, “Sensory subtraction in robot-assisted surgery: fingertip skin deformation feedback to ensure safety and improve transparency in bimanual haptic interaction,” *IEEE Trans. on Biomedical Engineering*, vol. 61, no. 4, pp. 1318–1327, 2014.
- [5] W. McMahan, J. Gewirtz, D. Standish, P. Martin, J. A. Kunkel, M. Lilavois, A. Wedmid, D. I. Lee, and K. J. Kuchenbecker, “Tool contact acceleration feedback for telerobotic surgery,” *IEEE Trans. on Haptics*, vol. 4, no. 3, pp. 210–220, 2011.
- [6] C. Pacchierotti, D. Prattichizzo, and K. J. Kuchenbecker, “A data-driven approach to remote tactile interaction: from a BioTac sensor to any fingertip cutaneous device,” in *Proc. EuroHaptics*, Versailles, France, 2014.
- [7] N. Wettels and G. E. Loeb, “Haptic feature extraction from a biomimetic tactile sensor: force, contact location and curvature,” in *Proc. IEEE International Conference on Robotics and Biomimetics*, 2011, pp. 2471–2478.
- [8] C. Pacchierotti, F. Chinello, M. Malvezzi, L. Meli, and D. Prattichizzo, “Two finger grasping simulation with cutaneous and kinesthetic force feedback,” *Haptics: Perception, Devices, Mobility, and Communication*, pp. 373–382, 2012.